

# Water Quality Monitoring System for Temperature, pH, Turbidity, DO, BOD, and COD Parameters Based on Internet of Things in the Garang Watershed

Syafrudin<sup>1</sup>, Anik Sarminingsih<sup>1</sup>, Henny Juliani<sup>2</sup>, Mochamad Arief Budihardjo<sup>1\*</sup>, Annisa Sila Puspita<sup>3</sup>, Shafa Auliya Arlin Mirhan<sup>3</sup>

<sup>1</sup> Departement of Environmental Engineering, Faculty of Engineering, Universitas Diponegoro, Jalan Prof. Soedarto, SH, Semarang, 502775, Indonesia

<sup>2</sup> Faculty of Law, Universitas Diponegoro, Jalan Prof. Soedarto, SH, Semarang, 502775, Indonesia

<sup>3</sup> Environmental Sustainability Research Group, Departement of Environmental Engineering, Faculty of Engineering, Universitas Diponegoro, Indonesia

\* Corresponding author's e-mail: m.budihardjo@ft.undip.ac.id

## ABSTRACT

Water has recently become a final disposal site for wastewater. Land use has evolved with the global population growth and is generally transformed into settlements and industrial areas. These land use changes could potentially increase wastewater generation from both domestic and non-domestic activities. The Garang watershed, one of the watersheds in Central Java, flows through the Semarang Regency, Kendal Regency, and Semarang City. This study analyzed the water quality conditions in the Garang watershed and designed a real-time water quality monitoring system. The methods used in this study included SWMM modeling, the national sanitation foundation water quality index (NSF-WQI), and the internet of things. Samples were collected from 10 points in the Garang Watershed, with a sampling frequency of five times at each point. The results of the data analysis demonstrated that the differences in land use resulted in varying water parameter levels. The results of the SWMM modeling demonstrated an acceptable model value (NOF between 0 and 1). On the other hand, the WQI analysis results demonstrated that the quality status at the Garang watershed is “medium” at nearly all location points. The designed real-time water quality sensor tool successfully transmitted water quality data online and in real-time, particularly for temperature, pH, turbidity, and DO. This water quality monitoring system offers a variable percentage error value, with the pH sensor ranging between 0.16% and 9.86% and the temperature sensor ranging between 0.64% and 1.72%.

**Keywords:** water quality index, SWMM, monitoring system, internet of things.

## INTRODUCTION

Water is one of the most important components of all life forms (Ewaid, Abed, Al-Ansari, & Salih, 2020). Humans, animals, and plants cannot survive in the absence of water. It can be obtained from a variety of sources, such as surface water, groundwater, and rainwater (Budihardjo et al., 2022). Rivers are currently the final disposal sites for wastewater in terms of water sources (Khan et al., 2020). Human activity has, consequently had a substantial impact on river water quality (Akhtar et

al., 2021). Land use has evolved over the years to maintain the stability with increasing global population, with the land typically being transformed into settlements and industrial areas (Ellis, 2021; Tong et al., 2023). These land-use changes may potentially increase wastewater generation from both domestic and non-domestic activities (Kumar Sarangi et al., 2023).

Semarang, the capital city of Central Java, has a relatively dense population of 1.659.975, with a 0.22% growth rate from 2020 to 2022 (BPS, 2022). One of the watersheds in Semarang City is

the Garang watershed, comprising four sub-watersheds – the Upper Garang, Kripiki, Kreo, and Lower Garang (Hanafi & Pamungkas, 2021). The Garang watershed flows through the Semarang Regency upstream, and the Kendal Regency and Semarang City downstream. The Garang watershed provides numerous benefits to human life – the upstream section serves as a runoff reservoir. In contrast, the downstream section is used as a raw water resource and a flood control canal. The Jatibarang Dam plays a significant role in flood management specifically in the Kreo sub-watershed (Huda et al., 2019).

However, various problems have occurred along the Garang watershed due to the changes in land use (Dibaba, Demissie, & Miegel, 2020). One of the largest changes in land use occurred around the upper watershed, formerly used as a protected area and is currently being converted into a settlement and an agricultural area. Several industries have developed in this area, including food and beverage packaging, textiles, steel, pharmaceuticals, and hotels. Waste is, consequently, abundant in agriculture, domestic households, and industrial operations in the upstream of the Garang watershed. The overflow of wastewater in the watershed results in the degradation of water quality, as indicated by increased turbidity, BOD, and COD, as well as decreasing DO. This was reinforced by the water quality data of the Garang River from January 2020 to 2022, which were obtained from the PDAM Tirta Moedal Semarang. The NTU level increased to 40 NTU in 2021, whereas it increased to 1,3 and 1,6 mg/L from 2021 to 2022.

The internet of things (IoT) can generally work on multiple platforms and can be used in various applications (Deng et al., 2021). It has inspired the development of numerous technologies, including water quality monitoring systems (Gulati et al., 2022). In this study, a water quality monitoring tool based on the internet of things was developed specifically for the Garang watershed. This tool provides a water quality measurement system for the river continuously and in real-time. The measurement results of the system were integrated into a publicly accessible website. Unlike the previously developed internet of things-based water quality monitoring system, this study also analyzed water quality against the land-use changes occurring around the Garang Watershed. SWMM modeling may be a better method to assess the correlation

between the Garang watershed quality and land use change. SWMM is a modeling software that can simulate rainfall and dynamic runoff for single occurrences, as well as long-term runoff quantity and quality studies (McDonnell et al., 2020). Along with the development of technology that is currently underway in the Industrial Revolution 4.0, the model validation method will be utilized as a design for monitoring the water quality of the Garang Basin River in real time based on the IoT. IoT refers to the process of connecting various sensors in the environment to nets (Kumar et al., 2019). As a result, the use of IoT will make the real-time monitoring of water quality significantly easier (Smys, 2020).

This study also explored the design of a real-time Garang watershed quality monitoring tool model based on the IoT. This study analyzed the water quality of the Garang Watershed during the rainy season without any prior treatment. The observed parameters consider the sources of pollutants entering the Garang Watershed, dominated by domestic, industrial, and agricultural activities, including temperature, pH, turbidity, DO, BOD, and chemical oxygen demand COD. The parameters that are monitored using the IoT-based monitoring tool are limited to those that can be monitored directly in real-time, including temperature, pH, turbidity, and DO.

This paper discussed the analysis of the water quality conditions in the Garang Watershed using SWMM modeling, analysis of the water quality index status, and the design of an Internet of Things-based real-time water quality monitoring tool model (more effective and efficient monitoring, evaluation and control of water quality) (Ijadaradar & Chatterjee, 2018) in the Garang Watershed which is equipped with tool monitoring data calibration. This paper is structured into several sections, including introduction, methodology, results, discussion, and conclusion. This study is expected to provide a recommendation for water quality monitoring points in the Garang watershed in real time to identify and analyze any significant change in water quality. This study is additionally expected to be one of the materials for the advancement of land use and water quality modeling technology using SWMM software as the basis for designing a model of real-time water quality monitoring tools based on the IoT, particularly in the Garang Watershed.

## METHODS

### Materials

The water samples at the Garang watershed were collected at 10 locations across the four Garang sub-watersheds – the Kripik, Kreo, Garang upstream, and Garang downstream sub-watersheds. Several parameters including temperature, pH, turbidity, and DO were tested based on these water samples, considering these parameters represent river water quality and require testing in real-time. Furthermore, the BOD and COD are additional parameters tested considering these parameters are generally contained in the wastewater from domestic, industrial, and agricultural activities that flow through the Garang Watershed (Sharma et al., 2022).

Several supporting tools were used to sample the water in the Garang watershed, including the Global Positioning System (GPS) which is used to determine the position of sampling coordinates, a water sampler to assist the water collection process, containers in the form of sterile jerry cans with a volume of 1 liter equipped with labels as storage of water samples for physical and chemical parameters,

roll meters to measure the width and depth of the river, and buckets to collect water from the sources that are difficult to reach (Specht, 2020; Tsuji et al., 2019). A cool box was additionally used to store the samples to ensure that the condition of the sample did not change. Several parameter-measuring devices were provided to directly measure certain parameters, including a digital pH meter for measuring pH, a thermometer for measuring temperature, a nephelometer for measuring water turbidity, and a DO meter for measuring DO parameters (Uddin et al., 2021). In addition to these parameters, river flow velocity was measured using a current meter (Pasika & Gandla, 2020). Sampling was performed ten times with different location coordinates, as presented in Table 1. A total of five measurements were recorded five times based on 10 sampling points.

In addition to water quality, discharge data were also utilized, which was obtained based on the rating curve. Water discharge is controlled by the flow rate and cross-sectional area (Dong et al., 2020). The rating curve demonstrates the correlation between the flow rate and water level (Xiang & Demir, 2020). The water discharge of the Garang Watershed was, therefore, determined at each water level interval.

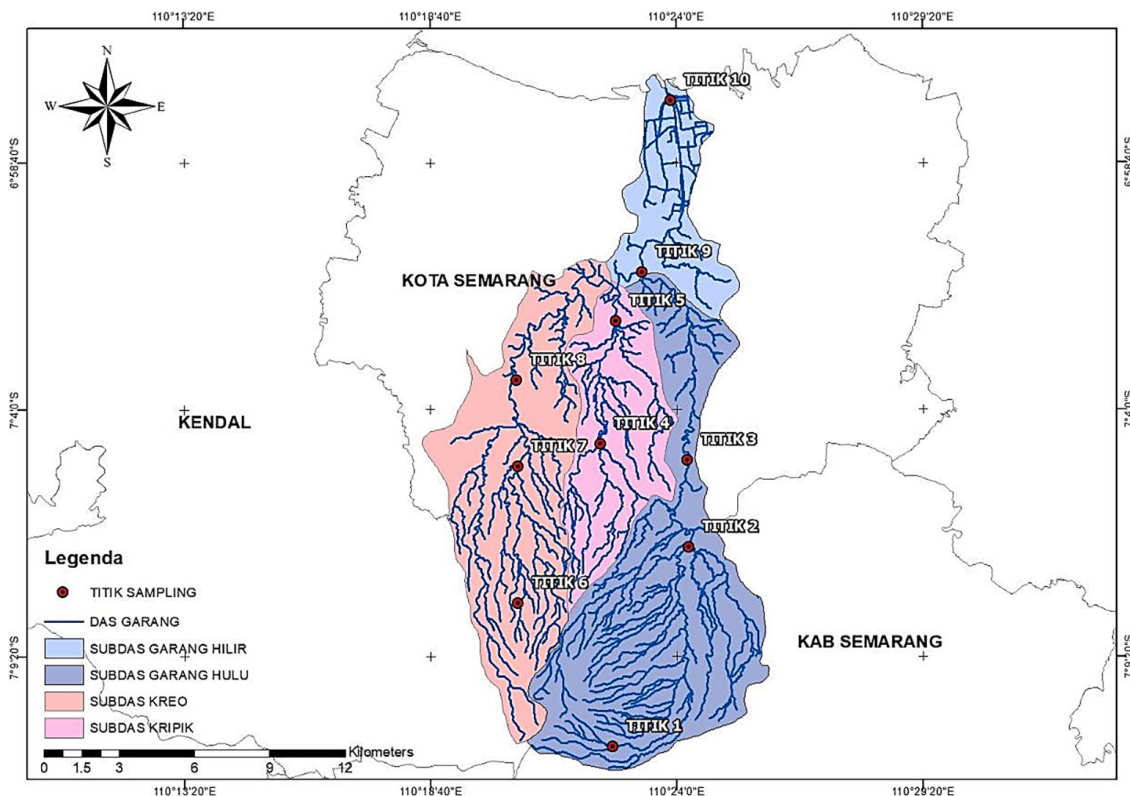


Figure 1. Sampling point location

**Table 1.** Sampling point location

No	Sampling point	Coordinate	Description
1	Point 1 (Upstream) located in Dusun Lempuyangan	7°11'16.4" S 110°22'36.9" E	Point 1 is located in the Garang Sub-upperstream was chosen since there are still few activities along the river, hence no or minor pollution has occurred.
2	Point 2 is located in Suwaktu, Village Bandarjo, Sub-district West Ungaran, Semarang Regency	7°06'57.4" S 110°24'16.2" E	Point 2 was chosen because of the presence of settlement activities around the location so that it is located in a location that has received sewage.
3	Point 3 is located on Jl. Tanah Putih II, Pudakpayung, Banyumanik District, Semarang City, Central Java Central	7°05'04.6" S 110°24'14.6" E	Point 3 was chosen because it has forest and plantation land use mixed land use. At this point allows for self purification
4	Point 4 is located in Jl. Gunungpati Raya, Gunung Pati District, Semarang City	7°04'43.6" S 110°22'21.2" E	Point 4 was chosen because of the presence of settlement activities around the location therefore it is located in a location that has received sewage.
5	Point 5 is located in Sukorejo Village, Gunung Pati District, Semarang City	7°02'04.7" S 110°22'41.9" E	Point 5 was chosen because of the presence of agricultural activities around the location therefore it is located in a location that has received sewage.
6	Point 6 is located in Jombon, Medono Village, Boja sub-district, Kendal Regency	7°08'10.1" S 110°20'34.3" E	Point 6 is located in the Garang Sub-upperstream was chosen since there are still few activities along the river, hence no or minor pollution has occurred.
7	Point 7 is located in Gunung Pati District, Semarang City	7°05'13.3" S 110°20'34.1" E	Point 4 was chosen because of the presence of settlement activities around the location therefore it is located in a location that has received sewage.
8	Point 8 is located in Sadeng, Gunung Pati District, Semarang City	7°01'50.4" S 110°21'32.8" E	Point 8 was chosen because the location of the river after Jatibarang dam.
9	Point 9 is located in Tugu Suharto Bridge, Bendan village, Gajahmungkur subdistrict, Semarang City	7°01'01.1" S 110°23'16.0" E	Point 9 was chosen because it is meeting point between the Garang Hulu, Kreo River and Kripik River.
10	Point 10 (downstream) is located in Yos Sudarso Bridge, North Semarang District, Semarang City	6°57'18.4" S 110°23'53.7" E	Point 10 was chosen because is the downstream of the Garang watershed and the accumulation of pollutants that flow from upstream to downstream.

## Analytical methods

SWMM is a software that is used to analyze land use against the quality of the Garang Watershed, especially in terms of DO, BOD, and COD (Hussain et al., 2022). Modeling simulation using SWMM generates tables and graphs of the correlation between pollutant concentration and water discharge in three different conditions, such as existing conditions, maximum rain, and minimum rain. Modeling with the SWMM begins with the division of sub-catchments. The Garang Watershed is divided into sub-catchments based on the value of land development and the movement of rainwater runoff. The division resulted in ten sub-catchments, where each represented one sampling point. A network model was created by entering the hydrological and hydraulic data (Andimuthu et al., 2019). The sub-catchment data and rain gauges were included in the new hydrological datasets. The addition of rain gauges at certain points as rainfall data in the form of intensity, volume, and time interval for one or sub-catchment areas in the Garang Watershed. The hydraulic data that must be provided comprises nodes in the form of junctions and outfalls, as well as links in

the form of conduits. The junctions are interconnected through conduits, where the flow moves from a junction at a certain elevation to a junction at a lower elevation. The entire network will encounter an outfall.

The Garang Watershed has different land use types, which can affect the river quality considering they are related to the leaching of pollutants on land use during wet weather events; they, therefore, have various event mean concentration (EMC) values (Wang et al., 2021). EMC is the concentration of specific pollutants contained in stormwater runoff resulting from a particular land use type within the specific land use type within the watershed (Puspita et al., 2023). EMC represents the average pollutant concentration for a rainfall event. The EMC during sampling is the ratio of the total pollutant mass to the total runoff volume during an event (Perera, McGree, Ego-dawatta, Jinadasa, & Goonetilleke, 2021).

Model evaluation was performed using the root mean square error (RMSE) method as a form of validation to measure the accuracy level of the modeling work. RMSE is the most frequently used model to measure the quality of alignment between existing data and the

hypothesized model (Prasetyo et al., 2021). Additionally, a water quality index calculation using the method by the national sanitation foundation (NSF-WQI) was used to analyze the quality of the Garang Watershed. This method simplifies the values of six measured parameters – temperature, pH, turbidity, DO, BOD, and COD – into a single rating that represents the overall water quality (Wiranto, 2019).

A monitoring system integrated with sensors was designed to monitor the water quality of the Garang watershed in real time. The sensors recorded real-time temperature, pH, turbidity, and DO measurements every 30 min. The data from the sensors were recorded and processed using an Arduino Leonardo microcontroller with LattePanda V1. These monitoring tools use the Internet of Things (IoT) for data storage; water quality data can, therefore, be retrieved in real time over the Internet. The monitoring system was designed for several nodes in a single area, where the system was intended to accept data from several pre-set river stations/locations. The primary framework of the station nodes comprises sensor-node modules, a master database, and a web server. AutoCAD was used in the system design process to construct the hardware and block diagram. The water quality data from the monitoring system were, however, compared with laboratory test results as a type of data calibration for the monitoring system outcomes.

## RESULT AND DISCUSSION

The planning area of the Garang Watershed covers a total of 20,792.89 Ha covering four sub-watersheds that are mostly comprised of dryland forest, secondary plantation forest, plantation, dryland agriculture, industry, settlement, open land, mixed dryland agriculture, and reservoirs. The differences in land-use patterns served as the basis for partitioning the Garang Watershed into 10 sub-catchments. Domestic, agricultural, and industrial wastes are consequently the primary sources of wastewater flowing through the Garang Watershed. The pollutant content of each wastewater source differed significantly (Pan et al., 2020). Domestic wastewater contains BOD and COD with emission rates of 53 and 101.6 grams/capita per day, respectively. Agricultural waste comprises only 70 g BOD per capita per

day. The amount of water discharged can, however, also affect temperature, pH, turbidity, and DO.

The water discharge flowing into the Garang Watershed significantly fluctuated and was also affected by weather variables. The discharge of each sub-watershed from upstream to downstream was found to be the highest. Among the 10 points of water sampling locations, the maximum discharge was located at point 8 precisely in the Kreo sub-watershed, Gunung Pati District, Semarang City, with a measured discharge of 18.76 m<sup>3</sup>/s.

The temperature of the Garang Watershed demonstrated a tendency to be higher when the discharge was higher. The entire watershed had a temperature range of 20–32 °C. The temperature rise may be affected by a variety of factors, including height, time, air circulation, cloud cover, and water flow. The increased temperature reduces the amount of oxygen dissolved in the water. Similar to the temperature, the pH levels in the Garang watershed were also relatively stable, ranging from 7.1–8.8. The highest pH level was located at point 10, where settlements dominated land usage. The toxicity of a chemical molecule may be affected by its pH value; as the pH increases, it leads to higher alkalinity and lower carbon dioxide. Meanwhile, the turbidity level in the Garang Watershed was affected by the surrounding land use. Turbidity levels are high in the areas where the land is used for agriculture (Tahiru et al., 2020). Farmers require the ground devoid of grass and other plants; therefore, when it rains, the empty gaps between plants are directly exposed to rain, resulting in erosion. The eroded soil is carried by the surface flow into the river, thereby increasing the turbidity of the water (Maruffi et al., 2022). The highest turbidity in the Garang watershed was found to be 838 NTU.

According to the water quality analysis of the Garang watershed, the DO content in the water decreased downstream of the river. The land around the river is particularly used for settlements and industries. Domestic waste discharge caused by community activities results in an increase in incoming organic matter, which can lower DO concentrations. The lower the DO content, the lower the river water quality. The lowest DO level in the entire Garang watershed was found to be 3 mg/L. This statistic falls short of the quality guidelines that require a minimum value of 6 mg/L. The DO concentration in the water was aligned with the BOD and COD levels. The high concentrations of BOD and COD

in water indicate the amount of organic matter that can be biologically degraded and the amount that is difficult to biologically degrade, comprising dead animals, plants, and domestic and industrial waste products (Suryawan et al., 2021). The highest BOD and COD concentrations in the Garang watershed were found to be in the agricultural, settlement, and industrial sectors. The water emissions generated from domestic and commercial activities near the river led to an influx of organic matter, thereby affecting the concentrations of BOD and COD, thus indicating a significant level of water pollution. The highest levels of BOD and COD in the Garang watershed were found to be 10.34 mg/L and 103.6 mg/L, respectively.

### Storm water management model

Water quality analysis commenced with the creation of a channel model along the Garang River watershed using the SWMM software. As presented in Figure 1, the SWMM modeling for analyzing water quality was developed by generating 10 sub-catchments, 11 junctions, eight land uses, three rain gauges, and pollutants such as DO, BOD, and COD. The land use type has an impact on river quality, considering it is related to

the leaching of pollutants during the rainy season and has varied EMC values (Soltaninia, Taghavi, Hosseini, Motamedvaziri, & Eslamian, 2023). EMC represents the concentration of specific pollutants in stormwater runoff from a particular land-use type within a watershed (Yazdi et al., 2021). This value is generated from the ratio of pollutant mass to the total runoff volume (Perera et al., 2021). Industrial and commercial land types have a higher percentage of impervious surfaces, allowing for the more effective transport of pollutants and runoff (Ghazavi et al., 2020). However, when open areas, forests, and land with dense vegetation cover were used, the concentrations of pollutants were found to be lower because of the reduced impervious surface area (Kafy et al., 2022). The EMC values for DO, BOD, and COD in the Garang watershed were then calculated at each location. The range of EMC values at each time throughout the 2-month calculation was found to be 3.66 mg/L – 6.23 mg/L for DO parameters, 1.88 mg/L – 8.52 mg/L for BOD, and 44.75 mg/L – 99.13 mg/L for COD. The interpretation of the details is presented in Table 2.

Observation point 1 was located in the upper reaches of the Garang watershed, an area dominated by forests. At this point, the DO concentrations from the SWMM modeling results

**Table 2.** Composite EMC value of each parameter

Titik	Month	DO	BOD	COD
1	1	5.5	3.09	53.89
	2	6.23	2.45	49.92
2	1	4.98	3.72	53.47
	2	4.92	3	51.71
3	1	5.1	3.38	51.9
	2	5.4	3.41	52.21
4	1	5.51	2.98	57.49
	2	5.27	4.34	50.41
5	1	6.05	4.99	52.23
	2	5.15	3.56	62.64
6	1	5.36	1.88	59.86
	2	5.66	3.26	54.2
7	1	4.99	5.01	45.89
	2	5.53	5.18	99.13
8	1	4.63	6.24	44.75
	2	5.25	5.17	72.48
9	1	4.88	8.52	91.05
	2	5.47	3.12	49.61
10	1	3.66	4.97	46.63
	2	4.16	4.76	61.71

ranged from 5.61 to 5.87 mg/L, which were not significantly different from the DO observations of 5.61 mg/L of 6.25 mg/L. The DO concentration at this point was quite high and increasing, and was found to be affected by the type of land use with little human activity. Rainfall also has an impact on the DO levels in water. According to previous research by Brontowiyono et al. (2022), the presence of wastewater entering the river may increase the aeration process by the increasing river flow rate. Increased aeration increased the DO levels. In terms of the BOD levels, the concentration of 2.07 mg/L–4.76 mg/L is close to the modeling results of 2.07 mg/L–2.99 mg/L based on the observation results. The observed COD levels demonstrated a tendency to increase when there was a decrease in discharge under field conditions, ranging from 47.79 mg/L–59.37 mg/L. However, in COD modeling, there was an increase in the COD concentration considering the simulated discharge tends to be stable within a range of 50.1 mg/L–52.46 mg/L.

Observation point 2 was located in an area that had begun to be influenced by anthropogenic activities considering it is dominated by settlements, covering 54.16% of the total catchment area comprising 1511.03 Ha. The DO concentrations at point 2 were lower than that at point 1. This was influenced by the type of land in the area, dominated by settlements. The runoff rate was, thus high, which increases the pollutant leaching rate from land to rivers (Muratoglu, 2020). Similarly, the BOD and COD values at point 2 were higher than those at point 1, considering the wastewater input from residential areas greatly contributed to the increase in BOD and COD.

Observation site 3 was located in an area where 34.60% of the total area was dominated by forests and 65.29% more has been altered by anthropogenic activities – settlements and agriculture. The SWMM DO concentrations demonstrated the results close to the observed DO values. Similarly, the BOD and COD concentrations from the modeling results were close to the field test values. The BOD and COD values at point 3 were almost the same as the BOD and COD values at point 2 considering both points comprised the same land use, which is predominantly used for settlement. However, the wastewater input from the settlements greatly contributed to the increases in BOD and COD (Cicero Fernandez et al., 2019).

Observation point 4 was located where 50.58% of the total area was dominated by

plantations, and the rest was comprised of settlement and agricultural activities. The modeled DO and BOD concentrations were relatively similar at this point. There were, however, instances when the modeling results were lower than the observations. This is due to the difference in discharge values because of the rain. This is supported by a previous study that stated that the observation model is related to rain. Rain can, therefore, lead to differences in the values of the modeling results with existing conditions (Costabile et al., 2020). In contrast, the modeled COD levels were lower than the observed COD levels.

Observation point 5 was located in an area where 63.02% of the total area was dominated by agriculture, and the rest by settlements and plantations. The modeled DO concentration showed the results that were close to the observed DO value. There was, however, a slight difference owing to the differences in discharge values with the existing conditions caused by rain. Similarly, the modeled BOD was greater than the existing BOD, considering the former experienced a small increase when the modeled discharge was relatively stable, in contrast to the observed BOD, which experienced a significant decrease due to the dilution of pollutants caused by rain (Corsita, 2021). Meanwhile, there was a considerable difference between the modeled and observed COD values. This is because the input COD concentration at junction 5 of the model was considered the average value of the COD observation for all recorded times and not at a particular hour. The modeled COD was, therefore, relatively stable.

Observation point 6 was located in an area where 78.80% of the total area was dominated by forests, and the rest was used for agricultural activities. The modeled DO concentrations demonstrated the results close to the observed DO values. There was, however, a slight difference observed between the modeled BOD and COD levels and the existing conditions, which occurred because of an increase in runoff from built-up land after rainfall (Pal et al., 2023).

Observation point 7 was located in an area dominated by agricultural land, plantations, forests, and settlements. The results of the data input for the inflow discharge (base flow) and base concentration were correct, while the modeled DO concentration demonstrated results close to the observed DO value. The modeled BOD level, however, exhibited a larger value owing to a small increase in the modeled BOD when the

modeled discharge was relatively stable (Asgari et al., 2020). On the other hand, the model demonstrated good results for COD, because it had a value that was close to the observed COD.

The land use around observation point 8 was almost the same as that around point 7 – dominated by agriculture, plantations, forests, and settlements. At this point, the observation results of DO were close to that of the DO model, whereas there were still differences observed for BOD and COD. This difference occurred because the model BOD tended to increase when the model discharge was relatively stable. In contrast, BOD only increased when the existing water flow rate increased in the test results (Ma et al., 2020).

Observation point 9 was located in an area where 53.31% of the total area was dominated by agriculture, and the rest by settlements and plantations. The results of the DO modeling were close to the conserved DO values. The modeling results of the BOD and COD levels were, however, still very different from the observation results owing to the water flow. Previous research has also shown that different water discharges in the SWMM model with existing conditions due to rain can affect the BOD and COD levels (Dwi Sholehah et al., 2019).

Observation point 10 was located downstream of the Garang watershed, where 92.45% of its total area was dominated by settlements, whereas the rest comprised plantations and industrial areas. The input data for the base flow and base concentration were correct in the modeling results. The results of DO, BOD, and COD modeling were, therefore, close to the observations. There was, however, a slight difference in that the result of the BOD model was higher than the observation result. This condition developed when the BOD value in the existing condition decreased as the discharge decreased, although the modeled BOD value only decreased slightly.

The root mean square error (RMSE) approach was used to assess the findings of water quality modeling with the SWMM simulation, followed by the calculation of the NOF. The acceptable value range based on the NOF value calculation is 0.0–1.0 (Hardyanti et al., 2023). On the basis of the calculation of RMSE and NOF from the results of water quality modeling for DO, BOD, and COD parameters with SWMM at the 10 sample point locations, most of the NOF values were found to be below 1, indicating that the model is acceptable. However, some results

demonstrated NOF values greater than 1, such as at points 4 and 6 for BOD parameters, and points 8 and 10 for COD parameters.

### Water quality index-national sanitation foundation

The NSF-WQI method requires the identification of the state of the water quality of the Garang watershed in each sub-catchment based on the findings of water quality monitoring using specific criteria. On the basis of the findings of the analysis, a graph was created of the results of the multiplication of the weight ( $W_i$ ) of each parameter that affected the water quality status with the quality index ( $L_i$ ) of the measurement results plotted against the pollution index curve. The total of all parameter  $W_i \times L_i$  values generates the value of the water quality status; the greater the  $W_i \times L_i$  value, the higher the water quality status.

Sub-catchment 1, dominated by dryland forest, was mostly classified as “medium” with a value range of 65.06–67.10; at certain times, the water status at point 1 may be classified as “good.” The improved water quality status was attributed to the higher DO parameter values and lower temperatures.

Sub-catchment 2, which includes the Bergas, East Ungaran, and West Ungaran subdistricts, has 54.16% of its land comprised of settlements, with the rest used for plantations, forests, and industries. Open spaces account for only 1.20% of the total area. The land use in sub-catchment 2 resulted in a “medium” water quality index in the area, with a value ranging from 64.73 to 56.54. The most dominant polluting parameters were found to be temperature and turbidity in this sub-catchment.

Point 3 represents the river flow output from sub-catchment 3, comprising the Banyumanik sub-district, Bandungan sub-district, West Ungaran sub-district, East Ungaran sub-district, Boja sub-district, Gunugpati sub-district, Sumowono sub-district, Bergas sub-district, and Limbangan sub-district. There were considerable fluctuations in the water quality at this point. The water quality rating at point 3, however, remained “medium” after five sample periods with the range of 54.87–67.68. These changes may be attributed to rainfall. The presence of rain causes an input of contamination loads from agricultural and plantation activities, considering that agriculture and

plantations are also the dominant land uses in this area besides settlements (Kondo et al., 2021).

Meanwhile, 50.58% of sub-catchment 4, which includes Gunungpati and West Ungaran subdistricts, is utilized for plantations, while 25.14% is used for settlement areas. Temperature was found to be one of the most dominant parameters in this sub-catchment. Water temperature also affects DO saturation—when the temperature is higher, the DO saturation concentration is lower. Turbidity is a key characteristic the values of which are heavily impacted by rain. Despite this, the sub-catchment 4 water quality index was found to be in the “medium” range.

Point 5 represents the river flow output from sub-catchment 5, comprising numerous areas with land use dominated by dryland agriculture and settlements, accounting for 56.35% and 28.08%, respectively. The accumulation of domestic and agricultural waste, combined with the presence of rain, has an impact on the water quality, resulting in a high turbidity level. As a result, the water quality index status was considered “bad” during rainy days, with the worst index value of 46.63. Conversely, the best index value at this time was 65.5, classified as “medium.”

Sub-catchment 6 comprises numerous settlements from the Boja subdistrict, with a total population of 218. According to the NSF-WQI analysis, sub-catchment 5 had a water quality index value ranging from 67.27 to 69.2. As a result, the water quality status was categorized as “medium”.

Sub-catchment 7 had a total population of 12,726 and included the subdistricts of Mijen, Boja, Limbangan, and West Ungaran. On the basis of the data analysis, temperature, and turbidity were determined to be the most important characteristics. Furthermore, rain increased the turbidity levels, surpassing water quality limits. However, the water quality status at point 7 was rated as “medium” at all sampling times, with values ranging from 55.63 to 64.72.

Point 8 represents the river flow output from sub-catchment 8, in which 412.52 ha (14.25% of the land area) is used as a settlement, and the rest is used for agriculture. From the calculation results obtained, the water quality status at point 8 is classified as “medium,” with water quality index values ranging from 54.91–67.3. The lowest index value was obtained after rainfall, thus increasing the turbidity of the water.

Point 9 is the river flow output from sub-catchment 9. The most dominant pollutant parameters at point 9 were determined to be BOD, turbidity, and temperature. In the calculation of the water quality index, a low sub-index value indicates high pollution of the water body. At this point, turbidity was high owing to rain, exceeding the quality standard. Similarly, the high concentration of BOD exceeded the quality standards. A high BOD concentration in water indicates a high level of water pollution originating from organic materials (Saadali et al., 2020). The organic matter content in water can originate from domestic waste due to human activities, as well as from

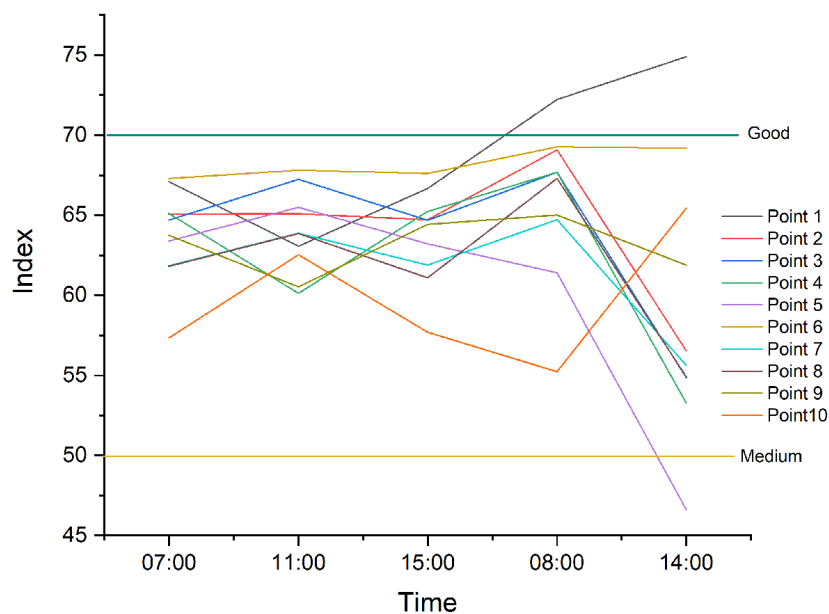


Figure 2. Water quality index

agricultural and plantation waste. The water quality index value in sub-catchment 9 ranged from 61.89 to 65.01, the water quality status being classified as “medium.”

The last sub-catchment, point 10, was comprised of plantations (4.44%) and industries (3.11%). According to the analysis, the dominant pollutants in sub-catchment 10 were determined to be turbidity and BOD. A high BOD concentration was produced due to the waste from activities along the Garang watershed. The location of sub-catchment 10, which is downstream of the Garang Watershed, causes higher pollution pressure. Nevertheless, the water quality index at point 10 was still classified as “moderate”, with values ranging from 55.24–65.44.

On the basis of the results of the NSF-WQI analysis of the 10 sub-catchments in the Garang watershed, almost every point was classified in the “medium” category overall. A summary of the index value of the entire Garang watershed sub-catchment is presented in Figure 2.

### Model design of real time water quality monitoring tool based on the Internet of Things

The Garang Watershed water-quality monitoring system was designed to measure four

parameters – temperature, pH, turbidity, and DO. The monitoring system was equipped with appropriate sensors that recorded quality data every 30 min using a microcontroller in the LattePanda V1 module for processing. Water quality data were subsequently transmitted in real-time to websites over the Internet (Huan et al., 2020). Users can obtain the monitoring results in the form of graphs and tables through the website, which can be accessed freely using mobile phones or computers.

A total of five sensors were used in planning the design of the monitoring tool, including the DS18B20 sensor, which was used to detect and monitor the temperature of the water – the SKU sensor SEN1283758, which detects and monitors pH levels; the sensor SKU: SEN0237, which detects and monitors DO levels in water; the sensor SKU: SEN0244, which detects and monitors the TDS levels; and the sensor SKU: SEN 0189, which detects and monitors turbidity levels (Ajith et al., 2020). The microcontroller processed and sent data from the sensor to the master data over the Internet (Perdana et al., 2020). As a power source, the monitoring tool stores and supplies electricity using a rechargeable battery with a voltage of 12 volts and current strength of 20 A.

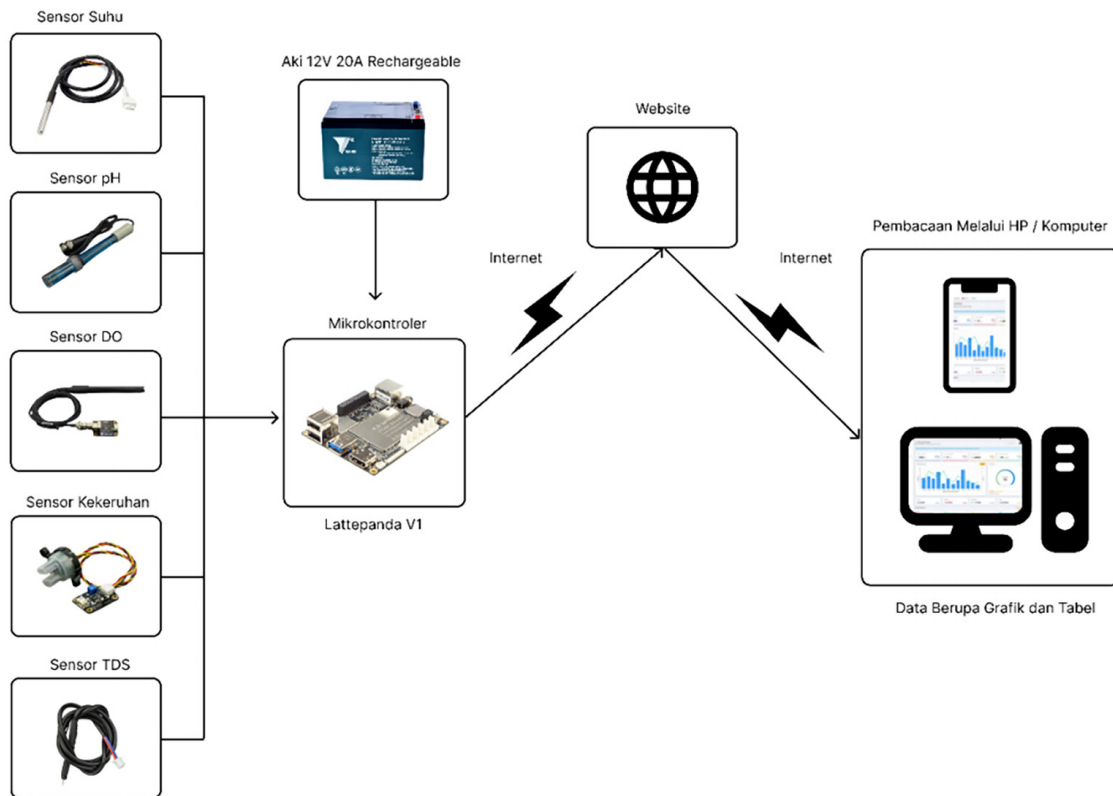


Figure 3. Diagram block online monitoring water quality system

**Table 3.** Specifications of the tools used

Component	Specification
Microcontroller	<p>LattePandaV1</p> <ul style="list-style-type: none"> <li>- Intel Cherry Trail Z8350 Quad-Core Processor</li> <li>- Base Frequency : 1.44GHz (1.92Hz Burst Frequency)</li> <li>- Operating System : Windows 10 Home Edition</li> <li>- RAM : 4GB DDR3L</li> <li>- Storage Capacity : 64GB</li> <li>- GPU : Intel HD Graphics, 12 EUs @200-500Mhz, single channel memory</li> <li>- USB 3.0 x 1, USB 2.0 x 2</li> <li>- Wi – Fi 802.11n 2.4G</li> <li>- Bluetooth 4.0</li> <li>- Intergrated Arduino Co-processor : ATmega32u4 (Arduino Leonardo)</li> <li>- Video Output : HDMI and MIPI-DSI</li> <li>- Onboard touch panel overlay connector</li> <li>- Support 100Mbps Ethernet</li> <li>- Intel Processor GPIO x 20</li> <li>- Voltage : 5V @2A</li> <li>- Board Dimension : 88 x 70 mm</li> <li>- NET Weight : 55g</li> <li>- Gross Weight : 100g</li> </ul>
Battery	<p>Motorcycle accumulator 12V 20A</p> <ul style="list-style-type: none"> <li>- Capacity : 20AH</li> <li>- Dimension : 180 x 78 x 172 mm</li> <li>- Terminal Size : D7Baterai SMT Power SMT1220 12V 20AH</li> <li>- Technology : Sealed Acid</li> <li>- Voltage : 12V</li> <li>- Terminal Type : Deep Cycle Battery</li> <li>- NET Weight : 7kg</li> </ul>
Temperature Sensor	<p>DS18B20</p> <ul style="list-style-type: none"> <li>- Supply Voltage : 3,3 V to 5 V</li> <li>- Temperature Range = -55 °C – 125 °C</li> <li>- Interface : Digital</li> <li>- Size : 22 x 32 cm</li> </ul>
PH Sensor	<p>pH Probe = SKU: 1283758</p> <ul style="list-style-type: none"> <li>- Type : Industrial Grade</li> <li>- Detection Range : 0 – 14</li> <li>- Temperature Range : 0 – 60 °C</li> <li>- Accuracy : ± 0,1pH (25 °C)</li> <li>- Response Time : &lt; 1 min</li> <li>- Probe Life : 7*24 hours &gt; 0,5 years (depending on the frequency of use)</li> <li>- Cable length : 500 cm</li> <li>- Probe Connector : BNC</li> </ul> <p>Signal Voltage</p> <ul style="list-style-type: none"> <li>- Supply Voltage : 3.3 – 5.5 V</li> <li>- Output Signal : 0 – 3 V</li> <li>- Signal Connector : PH2.0 – 3P.</li> <li>- Dimension : 42 mm x 32 mm.</li> </ul>
DO Sensor	<p>Dissolved Oxygen Probe = SKU : SEN0237</p> <ul style="list-style-type: none"> <li>- Type : Galvanic Probe</li> <li>- Detection Range : 0 – 20 mg/l</li> <li>- Temperature Range : 0 – 40 °C</li> <li>- Response Time : Up to 98% full response</li> <li>- Pressure Range : 0 – 50 PSI</li> <li>- Electrode Service Life : 1 year (normal use)</li> <li>- Maintenance Period : 1 -2 month (in muddy water); 4 -5 month (in clean water).</li> <li>- Cable length : 2 meters</li> <li>- Probe Connector : BNC</li> </ul> <p>Signal Voltage</p> <ul style="list-style-type: none"> <li>- Operating Voltage : 3.3 – 5.5 V</li> <li>- Output Signal : 0 – 3 V</li> <li>- Cable Connector : BNC</li> <li>- Signal Connector : Gravity Analog Interface (PH2.0 – 3P.</li> <li>- Dimension : 42 mm x 32 mm.</li> </ul>
Turbidity Sensor	<p>Turbidity Probe = SKU : SEN0189</p> <ul style="list-style-type: none"> <li>- Operating Voltage : 5V DC</li> <li>- Operating Current : 40mA (MAX)</li> <li>- Response Time : &lt;500ms</li> <li>- Insulation Resistance : 100M (Min)</li> <li>- Output Methode : Analog</li> <li>- Analog Output : 0 – 4,5V</li> <li>- Operating Temperature : 5°C – 90°C</li> <li>- Storage Temperature : -10°C – 90°C</li> <li>- Weight : 30g</li> <li>- Adapter Domention : 38 mm x 28 mm x 10 mm</li> </ul>

The water quality monitoring equipment has an LCD screen that performs similarly to a Windows 10 PC as well as an Arduino Leonardo microcontroller, Wi-Fi, and display record. The specifications used in the design of the monitoring tools are listed in Table 3.

A water quality monitoring system can be initiated by connecting the battery through a power socket; the microcontroller and LCD can, thus, be turned on. Before testing, the sensor was first immersed in water until it stabilized, and all the sensor parameters were read (Trevathan et al., 2021). By synchronizing the data to the Internet, the data obtained by the sensor will automatically be recorded in the database (Al Rasyid et al., 2016). Users will be able to obtain the water quality data for the Garang River watershed via the website after synchronizing with the Internet. Data readings from the device sensors are obtained every 30 minutes and displayed on the website in the form of graphs and tables that the user can download. The website contains the results of water quality readings and monitoring in the Garang watershed. The website has two features – home and acquisition logs. The home tool displays a graph of water quality readings from numerous stations at that time and from several locations, whereas

the acquisition log tool includes a data display in a tabular form that users can download.

Furthermore, data calibration was performed by comparing the measurement results of the pH and temperature sensors with those of pH standard solutions and thermometers to validate the data measured by the real-time water quality monitoring device (Burns et al., 2005). Data calibration aims to determine the error of a real-time water quality monitoring sensor (Pasika & Gandla, 2020). The percentage of error value is calculated during this calibration, which is the result of the difference between sensor readings and actual conditions compared with the number of trials (Wu et al., 2020). The pH sensor was calibrated by reading the pH value using standard solutions of pH 4, 7, and 9, and comparing the results with those of the pH sensor. The percentage errors for pH 4, 7, and 9 were found to be 0.16, 5.95, and 9.86%, respectively. The temperature sensor was calibrated in the laboratory by comparing the temperature measurements of the sensor device with those of a thermometer. A total of three water temperatures were used in this study – cold, standard, and hot. The percentage error value of the cold temperature reading was 0.64%, whereas the normal temperature

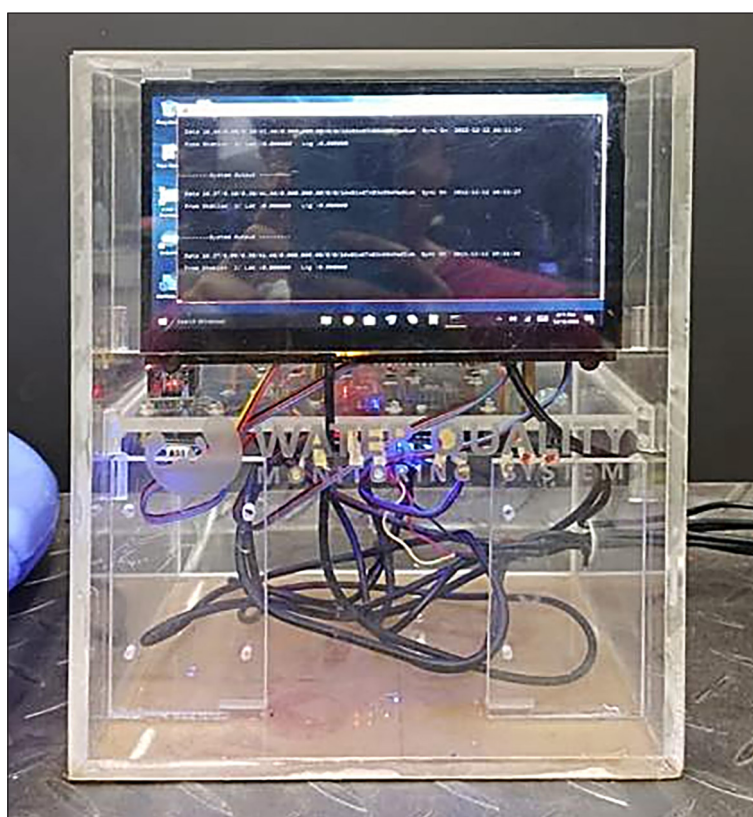


**Figure 4.** Front display of water quality monitoring device

sensor demonstrated an error percentage of 0.72% and that of the hot temperature was 1.73%.

There are several factors to consider in the operation and maintenance of real-time water quality monitoring devices based on the IoT system, particularly in monitoring temperature, pH, turbidity, and DO parameters, among others. Ultrasonic sensors may be employed for cleaning sensors, microcontrollers should be included in a box containing silica gel to maintain humidity, and direct sunlight should be avoided when operating the tool, considering excessive heat may harm its operation (Swamy & Kota, 2020). Furthermore, the DO sensor must be provided with a solution of NaOH when it is initially used to allow it to read the DO value of water (Akhter, Siddiquei, Alahi, Jayasundera, & Mukhopadhyay, 2021).

Several factors determine the position of real-time water quality monitoring equipment in the Garang watershed (Ramadhan et al., 2020). Several factors that determine system placement include the locations with a water quality status that changes significantly when sampling before and after rainfall, sites with river physical qualities that are not rocky, and locations that are easily accessible, allowing operators to monitor and maintain the tool more easily (Salam et al., 2019).

### Cost budget plan

Designing a real-time water quality monitoring system for the Garang watershed based on the Internet of Things is not just a matter of design; a budget plan is also required to meet the costs associated with the monitoring instrument (Campisi et al., 2020). A budget of Rp 21.760.500 was required as per the results of the cost calculation. This includes all the required tools, such as sensors, batteries, cables, SIM cards, websites, and support services for system assembly and installation.

### CONCLUSIONS

The changes in land use in each sub-catchment demonstrated a significant impact on the quality of water flowing into the Garang watershed. Settlements account for 32.31% of the land use, while agriculture accounts for approximately 25.25% of the total catchment area. Domestic and agricultural activities lead to significantly high concentrations of BOD and COD caused

by the presence of organic matter entering rivers via surface flow.

As per the results of the SWMM modeling, most of them showed that the model concentration value of each parameter at each observation point demonstrates an acceptable model value, although the BOD and COD parameters were declared invalid at points 4, 6, 8, and 10 considering the NOF value was greater than 1. Meanwhile, the range of EMC values in the Garang watershed was 3.66 mg/L–6.23 mg/L for DO, 1.88 mg/L–8.52 mg/L for BOD, and 44.75 mg/L–99.13 mg/L for COD. On the other hand, the results of the WQI analysis suggest that the water quality status of the Garang watershed is “medium” at nearly all location points. However, during a certain time, point 1 demonstrated “good” status, while point 5 was noted to be in “bad” condition.

The designed real-time water quality sensor tool successfully transmitted water quality data online and in real-time. Temperature, pH, turbidity, and DO were the parameters used to monitor the water quality. The data were transferred to a database using an Arduino Leonardo microcontroller and LattePanda V1. The website allows users to access real-time water quality data via computers or mobile water devices. This real-time water quality monitoring equipment offers a variable percentage error value, with the pH sensor ranging between 0.16% and 9.86% and the temperature sensor ranging between 0.64% and 1.72%.

### Acknowledgement

This research was gratefully supported by National Research Agency 2022 research funds, number 353/UN7.A/HK/XII/2022.

### REFERENCES

1. Ajith, J.B., Manimegalai, R., Ilayaraja, V. 2020. An IoT based smart water quality monitoring system using cloud. Paper presented at the 2020 International conference on emerging trends in information technology and engineering (ic-ETITE).
2. Akhtar, N., Syakir Ishak, M.I., Bhawani, S.A., Umar, K. 2021. Various natural and anthropogenic factors responsible for water quality degradation: A review. *Water*, 13(19), 2660.
3. Akhter, F., Siddiquei, H.R., Alahi, M.E.E., Jayasundera, K.P., Mukhopadhyay, S.C. 2021. An IoT-enabled portable water quality monitoring system

- with MWCNT/PDMS multifunctional sensor for agricultural applications. *IEEE Internet of Things Journal*, 9(16), 14307-14316.
4. Al Rasyid, M.U.H., Nadhori, I.U., Sudarsono, A., Alnovinda, Y.T. 2016. Pollution monitoring system using gas sensor based on wireless sensor network. *International Journal of Engineering and Technology Innovation*, 6(1), 79.
  5. Andimuthu, R., Kandasamy, P., Mudgal, B., Jegannathan, A., Balu, A., Sankar, G. 2019. Performance of urban storm drainage network under changing climate scenarios: Flood mitigation in Indian coastal city. *Scientific reports*, 9(1), 7783.
  6. Asgari, G., Shabanloo, A., Salari, M., Eslami, F. 2020. Sonophotocatalytic treatment of AB113 dye and real textile wastewater using ZnO/persulfate: Modeling by response surface methodology and artificial neural network. *Environmental research*, 184, 109367.
  7. BPS. 2022. Kota Semarang dalam Angka 2022.
  8. Brontowiyono, W., Asmara, A. A., Jana, R., Yulianto, A., Rahmawati, S. 2022. Land-use impact on water quality of the opak sub-watershed, Yogyakarta, Indonesia. *Sustainability*, 14(7), 4346.
  9. Budihardjo, M.A., Arumdani, I.S., Puspita, A.S., Ambariyanto, A. 2022. Improving Water Conservation at Universitas Diponegoro, Indonesia. *Journal of Sustainability Perspectives*, 2, 277-284.
  10. Burns, M.J., Nixon, G.J., Foy, C.A., Harris, N. 2005. Standardisation of data from real-time quantitative PCR methods—evaluation of outliers and comparison of calibration curves. *BMC biotechnology*, 5(1), 1-13.
  11. Campisi, T., Acampa, G., Marino, G., Tesoriere, G. 2020. Cycling master plans in Italy: The I-BIM feasibility tool for cost and safety assessments. *Sustainability*, 12(11), 4723.
  12. Cicero Fernandez, D., Expósito Camargo, J., Peña Fernandez, M., Antizar-Ladislao, B. 2019. Carex paniculata constructed wetland efficacy for stormwater, sewage and livestock wastewater treatment in rural settlements of mountain areas. *Water Science and Technology*, 79(7), 1338-1347.
  13. Corsita, L. 2021. Pengelolaan Waduk Kaskade Citarum Untuk Pengembangan Air Baku Infrastruktur Air Minum DKI Jakarta.
  14. Costabile, P., Costanzo, C., Ferraro, D., Macchione, F., Petaccia, G. 2020. Performances of the new HEC-RAS version 5 for 2-D hydrodynamic-based rainfall-runoff simulations at basin scale: Comparison with a state-of-the art model. *Water*, 12(9), 2326.
  15. Deng, Q., Goudarzi, M., Buyya, R. 2021. Fogbus2: a lightweight and distributed container-based framework for integration of iot-enabled systems with edge and cloud computing. Paper presented at the Proceedings of the international workshop on big data in emergent distributed environments.
  16. Dibaba, W.T., Demissie, T.A., Miegel, K. 2020. Drivers and implications of land use/land cover dynamics in Finchaa catchment, northwestern Ethiopia. *Land*, 9(4), 113.
  17. Dong, T.Y., Nittrouer, J.A., McElroy, B., Il'icheva, E., Pavlov, M., Ma, H., Moreido, V.M. 2020. Predicting water and sediment partitioning in a delta channel network under varying discharge conditions. *Water Resources Research*, 56(11), e2020WR027199.
  18. Dwi Sholehah, F., Samudro, G., Sarminingsih, A. 2019. Evaluasi kualitas air saluran pembuangan di sekitar segmen vi sungai garang menggunakan software swmm studi kasus: kecamatan gajahmungkur, kota semarang. Universitas Diponegoro.
  19. Ellis, E.C. 2021. Land use and ecological change: A 12,000-year history. *Annual Review of Environment and Resources*, 46, 1-33.
  20. Ewaid, S.H., Abed, S.A., Al-Ansari, N., Salih, R.M. 2020. Development and evaluation of a water quality index for the Iraqi rivers. *Hydrology*, 7(3), 67.
  21. Ghazavi, R., Imani, R., Esmali Ouri, A. 2020. Development and application of a new index-overlay method to assess urban runoff vulnerability to contamination (evaluation in the Ardabil city, Iran). *Arabian Journal of Geosciences*, 13, 1-12.
  22. Gulati, K., Boddu, R.S.K., Kapila, D., Bangare, S.L., Chandnani, N., Saravanan, G. 2022. A review paper on wireless sensor network techniques in Internet of Things (IoT). *Materials Today: Proceedings*, 51, 161-165.
  23. Hanafi, F., Pamungkas, D. 2021. Aplikasi Model Rusle untuk Estimasi Kehilangan Tanah Bagian Hulu di Sub Das Garang, Jawa Tengah. *Jurnal Geografi: Media Informasi Pengembangan dan Profesi Kegeografian*, 18(1), 30-36.
  24. Hardyanti, N., Susanto, H., Budihardjo, M., Purwono, P., Saputra, A. 2023. Application of response surface methodology (rsm) for optimisation of cod removal from tofu wastewater in an adsorption process using silica adsorbent. Paper presented at the IOP Conference Series: Earth and Environmental Science.
  25. Huan, J., Li, H., Wu, F., Cao, W. 2020. Design of water quality monitoring system for aquaculture ponds based on NB-IoT. *Aquacultural Engineering*, 90, 102088.
  26. Huda, A. S., Nugraha, A. L., Bashit, N. 2019. Analisis Perubahan Laju Erosi Periode Tahun 2013 Dan Tahun 2018 Berbasis Data Pengindraan Jauh Dan Sistem Informasi Geografis (Studi Kasus: Das Garang). *Jurnal Geodesi Undip*, 9(1), 106-114.
  27. Hussain, S. N., Zwain, H. M., Nile, B. K. 2022. Modeling the effects of land-use and climate change on the performance of stormwater sewer system using SWMM simulation: case study. *Journal of Water and Climate Change*, 13(1), 125-138.

28. Ijaradar, J., Chatterjee, S. 2018. Real-time water quality monitoring system. *International Research Journal of Engineering and Technology*, 5(3), 1166-1171.
29. Kafy, A.-A., Al Rakib, A., Fattah, M.A., Rahaman, Z.A., Sattar, G.S. 2022. Impact of vegetation cover loss on surface temperature and carbon emission in a fastest-growing city, Cumilla, Bangladesh. *Building and Environment*, 208, 108573.
30. Khan, R., Saxena, A., Shukla, S. 2020. Evaluation of heavy metal pollution for River Gomti, in parts of Ganga Alluvial Plain, India. *SN Applied Sciences*, 2(8), 1451.
31. Kondo, T., Sakai, N., Yazawa, T., Shimizu, Y. 2021. Verifying the applicability of SWAT to simulate fecal contamination for watershed management of Selangor River, Malaysia. *Science of the Total Environment*, 774, 145075.
32. Kumar, S., Tiwari, P., Zymbler, M. 2019. Internet of Things is a revolutionary approach for future technology enhancement: a review. *Journal of Big data*, 6(1), 1-21.
33. Kumar Sarangi, P., Subudhi, S., Bhatia, L., Saha, K., Mudgil, D., Prasad Shadangi, K., Arya, R. K. 2023. Utilization of agricultural waste biomass and recycling toward circular bioeconomy. *Environmental Science and Pollution Research*, 30(4), 8526-8539. <https://doi.org/10.1007/s11356-022-20669-1>
34. Ma, S., Kim, K., Chun, S., Moon, S.Y., Hong, Y. 2020. Plasma-assisted advanced oxidation process by a multi-hole dielectric barrier discharge in water and its application to wastewater treatment. *Chemosphere*, 243, 125377.
35. Maruffi, L., Stucchi, L., Casale, F., Bocchiola, D. 2022. Soil erosion and sediment transport under climate change for Mera River, in Italian Alps of Valchiavenna. *Science of the Total Environment*, 806, 150651.
36. McDonnell, B.E., Ratliff, K., Tryby, M.E., Wu, J.J.X., Mullapudi, A. 2020. PySWMM: the python interface to stormwater management model (SWMM). *Journal of open source software*, 5(52), 1.
37. Muratoglu, A. 2020. Grey water footprint of agricultural production: An assessment based on nitrogen surplus and high-resolution leaching runoff fractions in Turkey. *Science of the Total Environment*, 742, 140553.
38. Pal, S.K., Masum, M.M.H., Salaudhin, M., Hossein, M.A., Ruva, I.J., Akhie, A.A. 2023. Appraisal of stormwater-induced runoff quality influenced by site-specific land use patterns in the south-eastern region of Bangladesh. *Environmental Science and Pollution Research*, 30(13), 36112-36126.
39. Pan, C., Bao, Y., Xu, B. 2020. Seasonal variation of antibiotics in surface water of Pudong New Area of Shanghai, China and the occurrence in typical wastewater sources. *Chemosphere*, 239, 124816.
40. Pasika, S., Gandla, S.T. 2020. Smart water quality monitoring system with cost-effective using IoT. *Heliyon*, 6(7).
41. Perdana, R.H.Y., Hidayati, N., Yulianto, A.W., Firdaus, V.A.H., Sari, N.N., Suprianto, D. 2020. Jig detection using scanning method base on internet of things for smart learning factory. Paper presented at the 2020 IEEE International IOT, Electronics and Mechatronics Conference (IEMTRONICS).
42. Perera, T., McGree, J., Egodawatta, P., Jinadasa, K., Goonetilleke, A. 2021. Catchment based estimation of pollutant event mean concentration (EMC) and implications for first flush assessment. *Journal of Environmental Management*, 279, 111737.
43. Prasetyo, V.R., Lazuardi, H., Mulyono, A.A., Lauw, C. 2021. Penerapan Aplikasi RapidMiner Untuk Prediksi Nilai Tukar Rupiah Terhadap US Dollar Dengan Metode Regresi Linier. *Jurnal Nasional Teknologi dan Sistem Informasi (TEKNOSI)*, 7(1), 8-17.
44. Puspita, A.S., Budihardjo, M.A., Samadikun, B.P. 2023. Evaluating coconut fiber and fly ash composites for use in landfill retention layers. *Global nest journal*, 25(4), 1-7.
45. Ramadhan, A., Ali, A., Kareem, H. 2020. Smart water-quality monitoring system based on enabled real-time internet of things. *Journal of Engineering Science and Technology*, 15(6), 3514-3527.
46. Saadali, B., Khedidja, A., Mihoubi, N., Ouddah, A., Djebassi, T., Kouba, Y. 2020. Water quality assessment and organic pollution identification of Hammam-Grouz dam (Northeastern Algeria). *Arabian Journal of Geosciences*, 13(20), 1091.
47. Salam, M., Kabir, M., Yee, L., Khan, M. 2019. Water quality assessment of perak river, Malaysia. *Pollution*, 5(3), 637-648.
48. Sharma, P., Iqbal, H.M., Chandra, R. 2022. Evaluation of pollution parameters and toxic elements in wastewater of pulp and paper industries in India: A case study. *Case Studies in Chemical and Environmental Engineering*, 5, 100163.
49. Smys, S. 2020. A survey on internet of things (IoT) based smart systems. *Journal of ISMAC*, 2(04), 181-189.
50. Soltaninia, S., Taghavi, L., Hosseini, S.A., Motamedvaziri, B., Eslamian, S. 2023. The effects of antecedent dry days and land use types on urban runoff quality in a semi-Arid region. *International Journal of Urban Sciences*, 27(2), 215-238.
51. Specht, M. 2020. Statistical distribution analysis of navigation positioning system errors—issue of the empirical sample size. *Sensors*, 20(24), 7144.
52. Suryawan, I.W.K., Prajati, G., Afifah, A.S., Apriatama, M.R. 2021. Nh3-n and cod reduction in endek (Balinese textile) wastewater by activated sludge under different do condition with ozone

- pretreatment. *Walailak Journal of Science and Technology (WJST)*, 18(6), 9111-9127.
53. Swamy, S.N., Kota, S.R. 2020. An empirical study on system level aspects of Internet of Things (IoT). *IEEE Access*, 8, 188082-188134.
54. Tahiru, A.A., Doke, D.A., Baatuuwie, B.N. 2020. Effect of land use and land cover changes on water quality in the Nawuni Catchment of the White Volta Basin, Northern Region, Ghana. *Applied Water Science*, 10(8), 1-14.
55. Tong, D., Sun, Y., Tang, J., Luo, Z., Lu, J., Liu, X. 2023. Modeling the interaction of internal and external systems of rural settlements: The case of Guangdong, China. *Land Use Policy*, 132, 106830.
56. Trevathan, J., Schmidtke, S., Read, W., Sharp, T., Sattar, A. 2021. An IoT general-purpose sensor board for enabling remote aquatic environmental monitoring. *Internet of Things*, 16, 100429.
57. Tsuji, S., Takahara, T., Doi, H., Shibata, N., Yamana, H. 2019. The detection of aquatic macroorganisms using environmental DNA analysis – A review of methods for collection, extraction, and detection. *Environmental DNA*, 1(2), 99-108.
58. Uddin, M.G., Nash, S., Olbert, A.I. 2021. A review of water quality index models and their use for assessing surface water quality. *Ecological Indicators*, 122, 107218.
59. Wang, Y., Liu, X., Wang, T., Zhang, X., Feng, Y., Yang, G., Zhen, W. 2021. Relating land-use/land-cover patterns to water quality in watersheds based on the structural equation modeling. *Catena*, 206, 105566.
60. Wiranto, U.A. 2019. Pengaruh Musim Penghujan Terhadap Produktivitas Primer dan Status Mutu Kualitas Perairan Bendungan Lahor Kabupaten Malang Provinsi Jawa Timur. *ITN Malang*.
61. Wu, J., Hu, K., Cheng, Y., Zhu, H., Shao, X., Wang, Y. 2020. Data-driven remaining useful life prediction via multiple sensor signals and deep long short-term memory neural network. *ISA transactions*, 97, 241-250.
62. Xiang, Z., Demir, I. 2020. Distributed long-term hourly streamflow predictions using deep learning—A case study for State of Iowa. *Environmental Modelling & Software*, 131, 104761.
63. Yazdi, M.N., Sample, D.J., Scott, D., Wang, X., Ketabchy, M. 2021. The effects of land use characteristics on urban stormwater quality and watershed pollutant loads. *Science of the Total Environment*, 773, 145358.